# Nanoscale

Accepted Manuscript


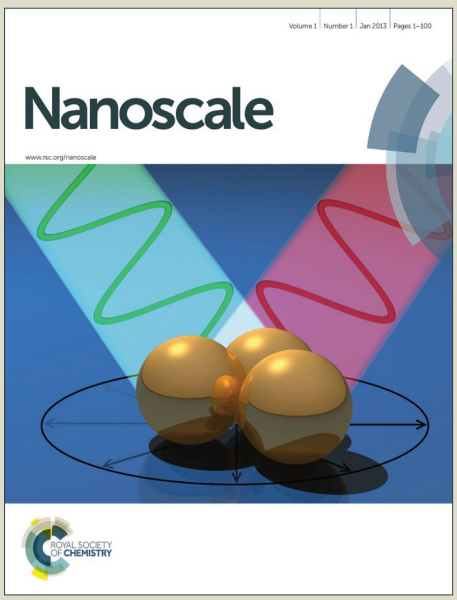



This is an *Accepted Manuscript*, which has been through the Royal Society of Chemistry peer review process and has been accepted for publication.

*Accepted Manuscripts* are published online shortly after acceptance, before technical editing, formatting and proof reading. Using this free service, authors can make their results available to the community, in citable form, before we publish the edited article. We will replace this *Accepted Manuscript* with the edited and formatted *Advance Article* as soon as it is available.

You can find more information about *Accepted Manuscripts* in the Information for Authors.

Please note that technical editing may introduce minor changes to the text and/or graphics, which may alter content. The journal's standard Terms & Conditions and the Ethical guidelines still apply. In no event shall the Royal Society of Chemistry be held responsible for any errors or omissions in this *Accepted Manuscript* or any consequences arising from the use of any information it contains.



ROYAL SOCIETY OF CHEMISTRY

www.rsc.org/nanoscale

Please do not adjust margins

Journal Name

ARTICLE

# Are vacuum-filtrated reduced graphene oxide membranes symmetric?

Received 00th January 20xx,
Accepted 00th January 20xx

DOI: 10.1039/x0xx00000x

www.rsc.org/

Bo Tang[a,†], Lianbin Zhang[a,†], Renyuan Li[a], Jinbo Wu[a], Mohamed Neijib Hedhili[b], and Peng Wang*[a]

Graphene or reduced graphene oxide (rGO) membrane-based materials have promised many advanced applications due to their exceptional properties. One of the most widely used synthesis method for rGO membranes is vacuum filtration of graphene oxide (GO) on a filter membrane, followed by a reduction, which shows great advantages such as operational convenience and good controllability. Despite vacuum-filtrated rGO membranes have been widely used in many applications, a fundamental question is overlooked: are the top and bottom surfaces of the membranes formed at the interfaces with air and with the filter membrane respectively symmetric or asymmetric? This work, for the first time, reports that the asymmetry of the vacuum-filtrated rGO membranes and discloses that the filter membranes' physical imprint on the bottom surface of the rGO membrane, which takes place when the filter membrane surface pores have similar dimension to GO sheets. This result points out that the asymmetric surface properties should be cautiously taken into consideration while designing the surface-related applications for GO and rGO membranes.

## Introduction

Graphene, an atom-thin layer of pure carbon, due to its exceptional properties, promises many unprecedented applications.[1, 2] However, the unpleasant reality is that the method of producing graphene with reasonable yield does not exist up to now.[3] So far, the scientific community has been relying on synthesis of graphene oxide (GO) sheet by chemical exfoliation of graphite,[3-5] followed by reduction of the GO to reduced GO (rGO) and it is the rGO that is widely used as the substitute to graphene in most of the exploratory research as rGO and graphene have shown similar physical and chemical properties.[6-8]

One added benefit of the GO to rGO method is that, GO, due to its charges, can be well dispersed in aqueous media, which facilitates many of solution based graphene processing.[9] Vacuum filtration, a conventional and simple laboratory technique of separating solids from fluids, has recently found its way into the emerging graphene field and established itself as an excellent method of making free-standing GO and rGO membranes.[10-20] In the vacuum filtration, GO solution is filtered through a membrane substrate under vacuum, and GO sheets, due to their big lateral size compared with the size of membrane pore, are retained and thus stack up on the membrane surface, forming a GO membrane. After proper chemical reduction, the GO membrane can then be converted into rGO membrane.[7, 18] Due to its simplicity, low-cost, and easiness to scale up, the vacuum filtration based graphene membrane fabrication has seen many applications in recent years, such as water desalination and purification,[12, 15, 16, 19, 20] energy storage,[14, 17] and oil-water separation.[19]

In a vacuum filtration system, commercial membrane filters are generally used as filtration medium. Would the filter membranes leave their imprints on the thus-prepared GO and subsequent rGO membranes? This question remained unanswered until very recently when Huang and coworkers discovered that some ionic species in the membrane filters could make their way into the overlying GO membranes and significantly change the stability of the GO membranes in aqueous media.[21] It was found that the ionic species coming from the filter membranes would bind with partially negatively charged GO sheets, which significantly increases the stability of the GO membrane.[21] This work helps explain inconsistency in the prior literature reports regarding the GO membrane stability in aqueous solution and shows that the membrane filters in the vacuum filtration may chemically affect the thus-prepared GO membranes.

It is believed that the above-mentioned chemical imprint would be insignificant when the GO membranes are reduced to rGO ones as the charges on the GO sheets would be minimized after reduction. However, there is another aspect of the filtration-based membrane preparation that has potential to impact the produced rGO membrane property, but

[a] Water Desalination and Reuse Center, Division of Biological and Environmental Science and Engineering, King Abdullah University of Science and Technology, Thuwal, Saudi Arabia. Email: Peng.wang@kaust.edu.sa
[b] Imaging and Characterization Laboratory, King Abdullah University of Science and Technology, Thuwal, Saudi Arabia.
† These authors contributed equally to this work.
Electronic Supplementary Information (ESI) available: [details of any supplementary information available should be included here]. See DOI: 10.1039/x0xx00000x

Nanoscale Accepted Manuscript



Please do not adjust margins

unfortunately has been overlooked in the past. A vacuum filtrated GO or rGO membrane has two surfaces, which are formed at different interfaces. Taking GO as an example, at the filter membrane and GO sheet interface, one GO surface, referred to as bottom surface hereinafter, is generated immediately upon direct contact between the GO sheets and the filter membrane substrate. The other surface, referred to as top surface hereinafter, is formed at a later stage upon the completion of the vacuum filtration and is at relatively free GO sheets and air interface. Would the top and the bottom surfaces of the resulted GO or rGO membranes have same or different chemical and physical properties or namely are the resulted GO or rGO membranes symmetric or asymmetric? More specifically, would the membrane filter substrate leave its physical imprint on the bottom surface of the rGO membranes?

To the best of our knowledge, the answers to these questions remain unexplored till now. Herein, this work is intended to find the answers to these questions by a carefully designed experiment whose results (1) disclose that vacuum filtrated rGO membranes indeed possess asymmetry and the filtration membrane does leave their physical imprint on the bottom surface of the resulted rGO membranes; (2) reveal that it is the filter membrane's physical imprint on the bottom surface of the rGO membranes that gives rise to the asymmetric properties of the rGO membranes; and (3) discover that it is the actual surface pore size of the filter membrane that controls its imprinting during the filtration, with the filter membrane imprinting taking place only when the filter surface pores have similar dimension to GO sheets. We believe that this work helps attract research attention onto the two surfaces of rGO membranes, which can be quite distinct in their properties, and it thus contributes a new avenue of varying properties of the two surfaces of rGO membrane for pre-designed applications.

## Experimental section

### Materials

The graphite powder, sodium nitrate, potassium permanganate, hydrochloric acid (HCl), and hydriodic acid (HI) were purchased from Sigma Aldrich™ (St. Louis, MI, USA). De-ionized water produced by Milli Q™ filtration system was used in all experiment. The hydrophilic PVDF membrane filter with a stated pore size of 0.22 μm and the hydrophilic Nylon membrane filter with a stated pore size of 0.45 μm were purchased from Millipore™. The AAO membrane filter with a pore size 0.20 μm and the filter paper were purchased from Whatman™. The 0.2 μm pore size PC membrane was purchased from Millipore™ and the 1 μm and 3μm PC membranes were purchased from Whatman™.

### Preparation of GO and rGO membranes

GO nanosheets were prepared from graphite by a modified Hummers' method.[22, 23] In order to fabricate GO membranes with difference thickness, a series of GO suspensions (~ 50 mL) with different GO mass ranging from 1 mg up to 10 mg were prepared by diluting the GO suspension prepared previously, then the diluted GO suspension was filtrated under vacuum by the membrane filters (e.g., PVDF, nylon, PC, AAO). Upon completion of the filtration, the intact GO/membrane filter complex was dried under room temperature overnight before the reduction. The reduction of GO to rGO was conducted in a sealed container where a glass bottle containing 2 mL of HI solution was placed uncapped to allow the HI vapor to evaporate. The container was sealed and kept in an oven at 90 °C for 2 h. A freestanding rGO membrane was ultimately obtained by peeling the reduced GO from the membrane filter.

### Fog harvesting experiment

A homemade fog collection system was used to evaluate the fog harvesting performance.[24] The rGO membrane sample (2.5 cm × 2.5 cm) was fixed on a glass substrate with the same size. The sample was hung with its surface perpendicular to the horizontal plane. A simulated fog flow (flow rate ~12 cm/s) was produced by a commercial humidifier and was captured by the vertically placed substrate surfaces. The experimental temperature is 21 °C and the relative humidity is around 90-95 %. The distance between the fog generator and the sample surface is ~9 cm. The captured water droplets were drained by gravity and were collected by a container located on top of the digital balance below the sample. A digital optical microscope (Dino-Lite) was used to record capture and movement behaviors of the water.

### Characterization

All contact angles data were measured on a dynamic contact analyzer OCA35 from DataPhysics. The droplet volume applied for static CA is 4 μL. For all advancing CA and receding CA, the volume of the droplet at the starting point is 4 μL and the dispensing and withdrawing speed is 0.5 μL/s. The surface morphology of the substrate was examined using scanning electron microscopy (FEI Quanta 600). Surface roughness analysis was carried out on atomic force microscopy (Agilent 5400 SPM). X-ray photoelectron spectroscopy (XPS) studies were carried out in a Kratos Axis Ultra DLD spectrometer equipped with a monochromatic Al Kα X-ray source (hν = 1486.6 eV) operating at 150 W, a multi-channel plate and delay line detector under a vacuum of ~$10^{-9}$ mbar.

## Results and discussion

### Preparation and characterization of vacuum-filtrated rGO membrane

A typical experimental procedure of making rGO membranes by a vacuum filtration is schematically presented in Fig. 1a. In

Nanoscale Accepted Manuscript


This journal is © The Royal Society of Chemistry 20xx

more details, a commercial hydrophilic polyvinylidene fluoride (PVDF) filter membrane with a stated pore size of 0.22 µm, a commonly used filter, was employed as filtration media in the vacuum filtration of GO suspension with a known GO mass (e.g., 10 mg) under a pressure difference of 730 mmHg. The GO suspension was undisturbed during the filtration. Upon the completion of the filtration, a dark brown GO membrane was formed (Fig. 1b left). The GO membrane along with the supporting PVDF filter membrane was air dried before being transferred to a sealed chamber where GO was reduced to rGO membrane by a hydroiodic acid (HI) vapor for 2 hour. Upon reduction, the coloration of the membrane changed from dark brown before the reduction to a metallic grey of the resulted rGO membrane (Fig. 1b right). A free-standing rGO membrane was readily obtained by peeling it off from the filter membrane. The thickness of the resulted rGO membrane was determined by the cross-sectional scanning electronic microscopy (SEM) images of the membranes. As plotted in Fig. 1c, the thickness of the rGO membranes increased linearly with the mass of the GO in the starting suspensions. The successful reduction of the GO to rGO was confirmed by the Fourier transform infrared (FTIR) and Raman spectroscopy measurements. After the HI treatment, the FTIR spectrum in Fig. 1d shows the significantly weakened or disappearance of oxygen containing functional group peaks, such as hydroxyl group at 3421 $cm^{-1}$, epoxy group at 1259 $cm^{-1}$, alkoxy group at 1065 $cm^{-1}$, carboxyl group at 1624 $cm^{-1}$ and carbonyl group at 1725 $cm^{-1}$.[23, 25] In the Raman spectrum, the GO membrane showed two prominent peaks at 1589 and 1365 $cm^{-1}$ (Fig. 1e), corresponding to the well-documented G and D bands.[26] After the HI treatment, the G and D bands were still present, but the intensity ratio of the D and G bands, $I_D/I_G$, increased dramatically, which was attributable to the increased number of isolated $sp^2$ domain after reduction. Moreover, consistent to the prior literature reports, the two surfaces (top and bottom) of the same GO or rGO membranes exhibited almost the same static water contact angles, with the two surfaces of the GO membranes having static water contact angles at ~34 ± 2° while those of the rGO ones at ~76 ± 5° (insets of Fig. 1b).[12, 27] These results further confirm the successful reduction of the GO to rGO as the chemical reduction reduces the polar functional groups of GO and it also seem to suggest that two surfaces (i.e., top and bottom surfaces) of the GO and rGO are symmetric.

**Asymmetry of the vacuum-filtrated rGO membranes**

However, some seemingly contradictory but interesting results were later observed. In one experiment, we soaked one of our rGO membranes in water and as soon as the membrane was pulled out of the water vertically, we immediately spotted a drastic difference in water behaviors on the two surfaces of the same rGO membrane (Fig. 2a, and *Supporting Information* Video S1): on the top surface, a dry surface with no water residue at all was obtained, while, in a sharp contrast, on the bottom surface of the same rGO membrane, there was a thin layer of water film, which adhered to the entire surface firmly. As a matter of fact, these seemingly contradictory wettability results are not against each other as they belong to two different domains: the static wettability versus dynamic wettability. The observed different wetting behaviors on the rGO membrane surfaces in our experiment while pulling the membrane out of the water fall into a dynamic wettability domain, which involves de-wetting of water from the membrane surfaces. Obviously, the rGO membrane exhibited asymmetrically dynamic wetting behaviors on its two surfaces.

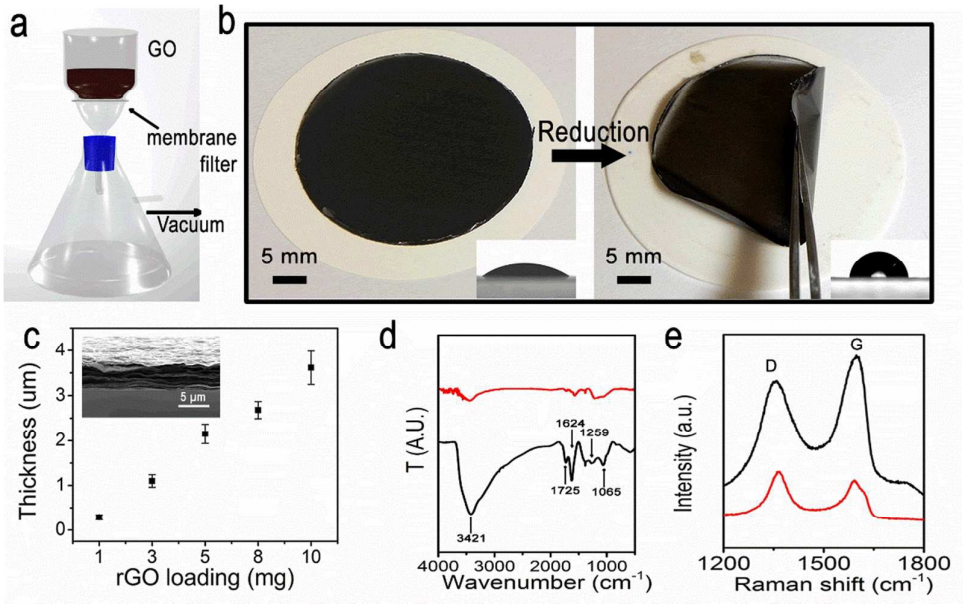


**Fig. 1**. GO and rGO membrane fabrication and characterization. (a) Setup for the vacuum filtration of the GO. (b) The image of the GO membrane (left) and rGO membrane (right) on top of the PVDF mem-brane filter with a stated pore size of 0.22 um. (c) The relationship between the mass of GO in the starting suspension and the thickness of the rGO membrane. Inset shows a cross-sectional SEM image of rGO membrane prepared from 10 mg GO. (d) The FTIR spectrum of the GO (black) and rGO membrane (red). (e) The Raman spectrum of the GO (black) and rGO (red) membrane.

Nanoscale Accepted Manuscript

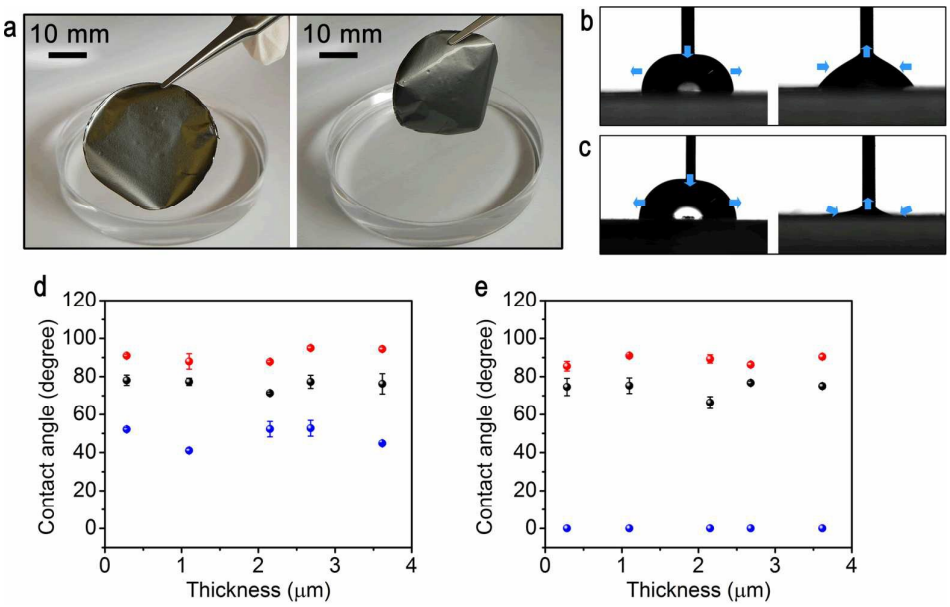


**Fig. 2**. Asymmetric dynamic wettability between two surfaces of rGO membrane prepared from PVDF membrane filter. (a) The digital photos of the rGO membrane top surface (left panel) and bottom surface (right panel) immediately after being taken out of water. (b) The advancing (left) and receding (right) angle of (b) the top and (c) the bottom surface of the rGO membrane. The dynamic and static wettability com-parison of (d) the top surface and (e) the bottom surface of the rGO membrane with different thickness. The red, black and blue spheres stand for advancing contact angle, static contact angle and receding contact angles.

In the dynamic wetting field, the researchers rely on advancing contact angle and receding contact angle measurements to provide important information.[28-30] Thus, for our rGO membranes produced on the PVDF membrane filters, we carefully measured their advancing and receding angles and found (1) there was no significant difference between the advancing angles of the two surfaces of the same rGO membrane (Fig. 2b, c left panels); (2) nevertheless, a drastic difference was observed on the receding angles between the two surfaces of the same rGO membrane, with the receding angle of the bottom surface measured to be 0˚ while that of the top surface at ~ 50° (Fig. 2b, c right panels). The receding angle of 0˚ at the bottom surface is an extreme and interesting case, which indicates the surface's capability to firmly hold the water and its unwillingness to let go of the water. This explains why there was a thin water film at the bottom surface of the rGO membrane after it was taken out of water. On the other hand, the 50˚ receding angle at the top surface indicates its general inclination to let go of the water. The drastically different water dynamic wetting behavior was consistently observed on the two surfaces of the free-standing rGO membranes with thickness ≥ 250 nm, as shown in Fig. 2d, 2e and Fig. S1. To facilitate discussion, from this point on, the rGO membrane samples with a thickness of 3.5 μm was used for focused discussions unless otherwise noted.

To find the cause of the asymmetric wetting behavior of the rGO membrane, the surface chemical composition and the surface structure on both the top and bottom surface of the membrane were then analyzed, which are believed to govern the wetting behaviors of solid surface.[31, 32] Both factors were looked at thoroughly in this study. First, X-ray photoelectron spectroscopy (XPS) measurement was conducted to examine the surface chemistry composition of the rGO membrane. It is believed that the magnitude of residual polar groups (e.g., C-O, C=O) on the rGO membrane partially affects its receding angle, with higher content of polar residue leading to smaller receding angle. Fig. 3 shows the XPS spectra of the GO (Fig. 3a) and both surfaces (top and bottom) of the rGO membrane after 2 hour HI treatment (Fig. 3b, c). Before reduction, the C 1s spectrum of the GO (Fig. 3a) was fitted with six components, located at 284.4, 285.1 eV, 286.4, 287.9, 288.9 eV, and 290.6 eV corresponding to the C=C ($sp^2$ hybridized carbon), C-C ($sp^3$ hybridized carbon), C–O–C/C–OH (epoxy and hydroxyl), C=O (carbonyl), O=C–OH (carboxyl) groups and π–π* shake-up satellite structure characteristic of conjugated systems, respectively.[18, 25, 33] Meanwhile, the dominant peak at 286.4 eV indicates that the most oxygen-containing functional groups in the GO were hydroxyl and epoxy groups. After HI treatment, there was an increase in both the intensity of $sp^2$ hybridized carbon and the intensity of π–π* shake-up satellite structure, in addition to the decrease of the intensity of hydroxyl and epoxy groups on both surfaces of the rGO membrane, demonstrating the successful reduction. The atomic ratio of C/O was estimated from the survey spectra for these samples. The dramatic increase of the C/O ratio for both surfaces of rGO membrane confirms the efficient removal of oxygen-containing functionalities by the HI reduction. The treatment by HI beyond 2 hours of the rGO membrane showed negligible change in the XPS spectra and the C/O ratio, indicating the sufficient reduction by 2 hour HI treatment (Fig. S2). However, the XPS spectra revealed some difference in the residual polar group contents on the two surfaces of the rGO membrane, with the bottom surface having higher polar residual content than that of the top surface (Fig. 3b, c). While

Nanoscale Accepted Manuscript


This journal is © The Royal Society of Chemistry 20xx

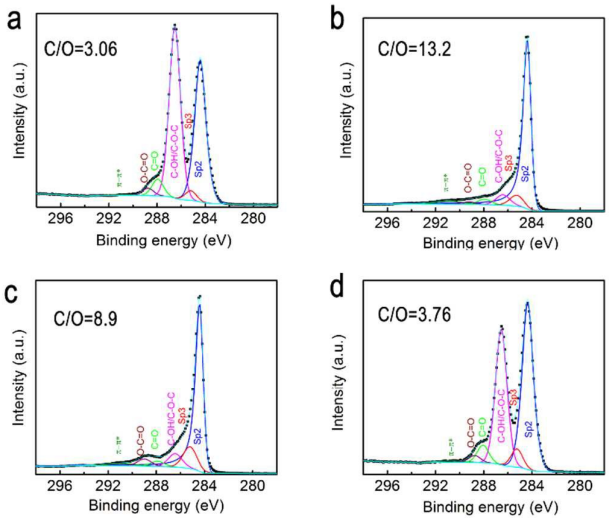


**Fig. 3**. C1s XPS spectra and C/O ratio analysis of GO and rGO membrane. (a) The GO, (b) the top surface, (c) the bot-tom surface of the rGO membrane, and (d) partially reduced (10 min HI treatment) top surface of the rGO membrane. The atomic ratios of C/O of these samples are 3.06, 13.2, 8.9, and 3.76, respectively.

2 hours was determined to be sufficient time to fully reduce the GO to rGO in this study, in one experiment, we kept the GO membrane in the HI vapor for only 10 minutes to purposefully prepare a partially reduced rGO membrane with a higher polar residual content than the fully reduced rGO membrane by 2 hour HI reduction (Fig. 3d). The result showed that the top surface of the partially reduced rGO membrane exhibited static and dynamic wettability similar to the top surface of the fully reduced one (Fig. S3). It is worth pointing out that the top surface of the partially reduced rGO membrane had much higher polar residual content (C/O ratio ~ 3.76) than the bottom surface of the fully reduced one (Fig. 3d), which implies insignificant role of surface chemistry difference in inducing different wetting behaviors and specifically different receding angles in this work. Thus, the above results make us believe that, although there is some difference in the polar residual content of the two surfaces of the rGO members, the difference is unlikely to be responsible to the drastically different wetting behavior on two surfaces of the same rGO membrane.

Next, the surface morphology on both surfaces of the rGO membrane was investigated. First, scanning electronic microscopy (SEM) images of the two surfaces of the rGO membrane were recorded and compared. As shown in Fig. 4a and 4b, the top surface of the rGO membrane showed generally smooth surface. Surprisingly, the bottom surface exhibited drastically different surface morphology, which was highly rough with many petal-like graphene sheets stretching out upright from the membrane surface (Fig. 4c, d). We took SEM images of the original PVDF and PVDF filter membrane after removing the overlying rGO membrane and found no rGO residue on the filter surface as well as in the PVDF membrane pores (Fig. 4e, f), which ruled out the possibility that these rGO surface microstructures were formed during delamination. Furthermore, atomic force microscopy (AFM) analysis was conducted in investigating the surface morphology of the rGO membrane. In conducting AFM measurements, the areas of 2.5 x 2.5 µm were scanned for both the surfaces, and root-mean-square roughness, $R_q$, which is considered as a reliable parameter in quantifying surface micro-roughness, was then calculated.[19, 29] The $R_q$ values of the top and bottom surfaces of the rGO membrane were calculated to be 31.4 nm and 63.4 nm respectively (Fig. S4). Clearly, according to the AFM analysis, the bottom surface assumed a rougher surface structure than the top surface of the same rGO membrane, consistent with the SEM imaging results. The relatively rougher structures on the bottom surface of the rGO membranes may allow the water to penetrate into the grooves and generate great resistance to the motion of the three-phase contact line, leading to lower receding angles.[29, 32] It is worth pointing out that the asymmetric morphology was also observed on the two surfaces of the GO membrane prepared on PVDF membrane without the HI reduction (Fig. S5).

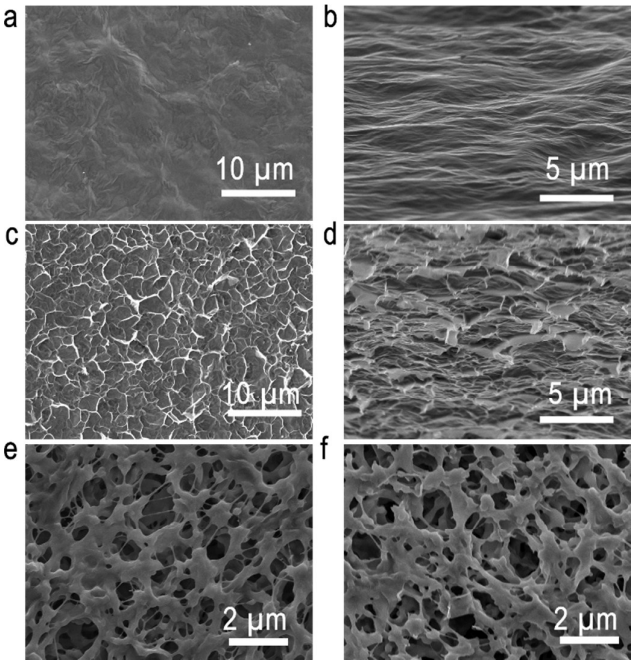


**Fig. 4**. SEM images of rGO and PVDF membrane filter. (a) Top and (b) tilt view SEM images of the top surface of the rGO membrane; (c) Top and (d) tilt view SEM images of the bottom surface of the rGO membrane; (e) SEM image of the original PVDF membrane with a stated pore size of 0.22 um; (f) SEM image of the PVDF membrane after delamination of the rGO membrane.

In order to further verify whether surface roughness, or more specifically, the surface petal-like microstructures in this work, is the true cause of the asymmetric wetting behaviors, we turned to polished silicon (Si) wafer, which is considered as a perfectly smooth surface, with an aim at producing rGO membrane with similar roughness and surface morphology on both surfaces. To prepare such a membrane, a GO suspension was dropped on top of the wafer and kept in a 40 °C convective oven for one week to evaporate water, followed by the same HI vapor reduction. A free-standing rGO membrane was ultimately prepared by carefully peeling it off from the Si

Nanoscale Accepted Manuscript

wafer surface. XPS measurements show that both the top and the bottom surfaces of the rGO membrane exhibited similar chemistry (Fig. S6). The SEM images (Fig. 5a, b) and AFM (Fig. S7) analysis show that both surfaces of the prepared rGO membrane were similarly smooth, with $R_q$ value being 23.6 nm and 20.1 nm on the top and bottom surfaces respectively. As expected, both the top and bottom surfaces of the rGO membrane produced from the Si wafer were smoother compared with those of the rGO membrane prepared on the PVDF membranes. At this point, it came as no surprise that both surfaces of this membrane left behind no water trace upon out of water contact. The advancing and receding angles of the top surface were measured to be 89 ± 1° and 49 ± 3°, while these of the bottom surface of the same rGO membrane produced on the Si wafer were 86 ± 1° and 33 ± 2° (Table 1). Thus, the fact that, with no difference in the surface roughness, the wetting behavior difference becomes insignificant, discloses that it is really the different surface roughness that makes the two surfaces of the same rGO membrane having different wetting behaviors.

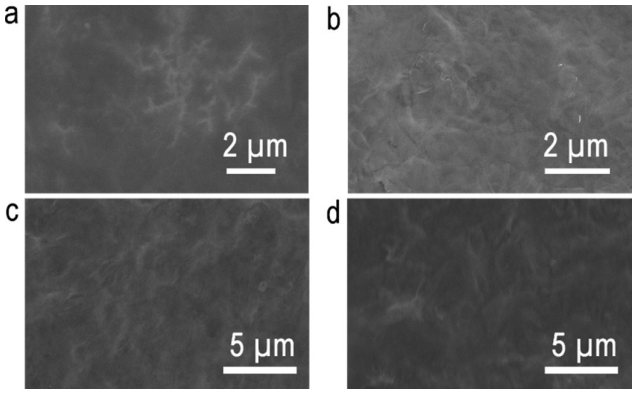


**Fig. 5**. SEM images of rGO membranes prepared on sili-con wafer and AAO membrane. (a) The top surface and (b) the bottom surface of the rGO membrane prepared on the Si wafer; SEM images of (c) the top surface and (d) the bottom surface of the rGO membrane prepared on the AAO mem-brane filter.

**Origin of the asymmetry of the vacuum-filtrated rGO membranes**

Having confirmed the role of surface roughness being responsible for the difference in water wetting behavior of the rGO membranes, efforts were then made in ascertaining whether the rough bottom surface of the rGO membrane could be reproduced if others filter membranes are used in the otherwise same process. In general, from the nature of the filter membrane preparation, filter membranes popularly used in vacuum filtration can be classified into two categories: phase-inversion-based polymeric filter membrane and anodic aluminum oxide (AAO). Nylon membrane, along with the PVDF one, falls into the first category.[34] We employed the nylon membrane (with a stated effective pore size of 0.45 μm) in the otherwise same vacuum filtration in this study and the results showed that the smooth top surface and rough bottom surface with petal-like microstructures could be well reproduced with the nylon filter membranes (Fig. S8). As expected, the bottom surfaces of the rGO membranes prepared on the nylon filter membranes possessed exactly the same water receding angle (i.e., 0°) as the ones prepared on the PVDF membranes. Next, AAO membrane, fabricated via anodization, was used for the preparation of the rGO membrane by the same process.[34] The AAO membrane has smooth surface and uniform and accurate pore size due to its fabrication process. In this work, an AAO membrane with 0.2 μm pore size was employed as filtration medium to produce rGO membrane. Very intriguingly, the SEM imaging (Fig. 5c, d) and AFM analysis (Fig. S9) revealed that the two surfaces of the so-produced rGO membrane were similarly smooth, with the $R_q$ values of the top and bottom surface being 30.3 nm and 37.8 nm respectively. In other words, with the AAO membrane being the filtration medium, the petal-like microstructures were not reproduced on the bottom surface of the rGO membrane. Not surprisingly, the thus-prepared rGO membrane showed no different wetting behavior between the top and bottom surfaces, with the static and dynamic contact angles all measured similar on the two surfaces (Table 1). Especially, the receding angles on the top and bottom surfaces of the thus-made rGO membrane were 41° ± 3° and 43° ± 2° respectively. In comparison, although both the polymeric filter membranes used in the study (i.e., PVDF and nylon) have a stated effective pore size of 0.22 μm and 0.45 μm, the surfaces of these filter membranes take on irregular and reticularly interconnected structures and their actual surface pore sizes are quite heterogeneous and diverse, ranging from several tens of nanometer to 2.0 μm for the PVDF membrane (Fig. 4e), and from 0.5 μm to 4.0 μm for the nylon one (Fig. S10). A careful comparison revealed that the dimension of periphery of the petal-like microstructures on the bottom surfaces of the rGO membranes was comparable to some of the surface pores of these polymeric filter membranes. These results now lead us to draw the conclusion that it is the filter membrane that induces surface petal-like microstructures on the bottom surface of the thus-prepared rGO membrane, provided that the filter membrane surface pore structure is so that it allows the entry of GO sheets into its surface pore space during vacuum filtration. Thus, the surface petal-like microstructures on the bottom surface of the rGO member are indeed physical imprints of the filtration membranes, leading to the asymmetry of the rGO membrane.

To further substantiate that the actual surface pore size of the filter membrane is the dominant factor that controls the filter membrane's imprinting on the bottom surfaces of the rGO membrane and thus the membrane asymmetry, track-etched polycarbonate (PC) membranes were rationally selected. The benefits of using the track-etched membranes are clear: (1) track etching process is capable of generating very uniform and well-controlled pore size; and (2) the pores are regular in shape.[34] We selected the PC membranes with pore sizes of 0.2 μm, 1.0 μm, and 3.0 μm (Fig. 6a-c) as filtration membranes while keeping the GO mass loading constant at 10 mg during vacuum filtration and compared the surface morphology and wettability behaviors of the two surfaces of the produced rGO membranes.

As expected, the SEM images showed smooth morphology on the top surfaces of all rGO samples as shown in Fig. 6a1, b1

Nanoscale Accepted Manuscript


This journal is © The Royal Society of Chemistry 20xx

Please do not adjust margins



Table 1. Properties and water wetting behaviors of the rGO membranes prepared from different filter membranes (substrate).

| | | Top surface of rGO membranes | | | | Bottom surface of rGO membranes | | | |
|---|---|---|---|---|---|---|---|---|---|
| Substrate | Actual pore size | Static contact angle | Advancing contact angle | Receding contact angle | Rq | Static contact angle | Advancing contact angle | Receding contact angle | Rq |
| PVDF | 0.5 ~4 μm | 76° ± 5° | 94° ± 1° | 45° | 31.4 nm | 75° ± 1° | 92° ± 2° | 0° | 63.4 nm |
| AAO | 0.2 μm | 77° ± 1° | 82° ± 2° | 41° ± 3° | 30.3 nm | 73° ± 1° | 85° ± 2° | 43° ± 2° | 37.8 nm |
| Si wafer | 0 | 72° ± 2° | 89° ± 1° | 49° ± 3° | 23.6 nm | 71° ± 1° | 86° ± 1° | 33° ± 2° | 20.1 nm |

and c1, which resulted in similar surface wettability on all top surfaces (Table 2). On the other hand, due to small pore size of the PC membrane, GO sheets, generally with size ranging from 0.5 to 5 μm (Fig. S11), are denied entry into the 0.2 μm pores and they end up stacking up on the membrane surface, leading to a petal-like microstructure-free smooth bottom surface of the rGO membrane as schematically illustrated in Fig. 6d. A smooth surface morphology was observed on the bottom surface of the rGO membrane prepared on the PC membrane with 0.2 μm pore size (Fig. 6a2, a3). However, when the PC membrane pore size was 1.0 μm, irregular petal-like microstructures were visible on the bottom surface of the rGO membrane (Fig. 6b2, b3). Interestingly enough, when the PC filter membrane pore size was 3.0 μm, round-shaped petal microstructures were clearly observed on the bottom surfaces of the rGO membranes and the sizes of the petal-like microstructures perfectly matched with the pore size of the corresponding PC filter membrane (Fig. 6c2, c3). The tilted-view SEM images of the bottom surfaces indicate that the height of the petal-like microstructures ranged from several ten nanometers to one micrometer. Such large surface pore size of these filter membrane allows the GO nanosheets with similar lateral dimension to partially penetrate, thus forming the petal-like structure (Fig. 6e). Different from the top surfaces of the rGO membranes,

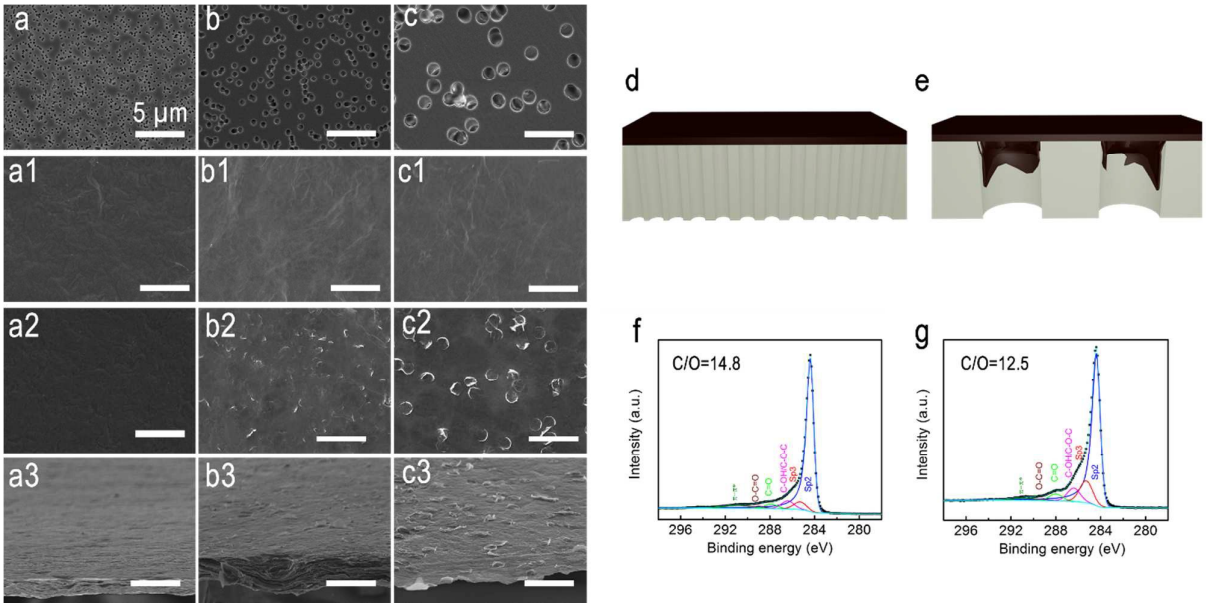


**Fig. 6**. Surface characterization of PC membrane and rGO membrane. SEM image of the PC membrane with a pore size of (a) 0.2 μm, (b) 1 μm and (c) 3 μm; top view of the top sur-face of the rGO membranes produced by (a1) 0.2 μm, (b1) 1 μm and (c1) 3 μm PC membranes; Top view of the bottom surface of the rGO membranes obtained by (a2) 0.2 μm, (b2) 1 μm and (c2) 3 μm PC membranes; Tilt view of the bottom surface of the rGO membranes fabricated on by (a3) 0.2 μm, (b3) 1 μm and (c3) 3 μm PC membranes. All scale bars corre-spond to 10 μm, except for that in (a). Schematic Illustration of GO stacking mechanism on different pore sized PC membrane, (d) 0.2 μm (e) 3.0 μm. C1s XPS spectra of the bottom surfaces of the rGO membrane obtained by PC membrane with a pore size of (f) 0.2 μm and (g) 3 μm.

Nanoscale Accepted Manuscript



Please do not adjust margins

Table 2. Water wetting behaviors of the rGO membranes prepared by the PC membranes with different pore sizes.

| | Top surface of the rGO membranes | | | Bottom surface of rGO membranes | | |
|---|---|---|---|---|---|---|
| Substrate | Static contact angle | Advancing contact angle | Receding contact angle | Static contact angle | Advancing contact angle | Receding contact angle |
| PC (0.2 μm) | 71° ± 1° | 89° | 44 ± 3° | 76° ± 4° | 91° ± 1° | 56° ± 1° |
| PC (1 μm) | 74° ± 3° | 90° ± 1° | 43° ± 2° | 71° ± 2° | 90° ± 1° | 32° ± 2° |
| PC (3 μm) | 72° ± 4° | 91° ± 1° | 47° ± 4° | 65° ± 3° | 84° ± 3° | 0° |

a clear and gradual transition with increasing PC filter membrane pore size was observed in the receding angles on the bottom surfaces of the rGO (Table 2). More specifically, a clear transition from a symmetry to asymmetry in the wetting behaviors of the both surfaces of the rGO membranes was obtained as the pore size of the PC filter membranes increased from 0.2 to 3.0 μm, with the receding angles on the bottom surface reduced to 0° at 3.0 μm PC filter membrane pore size. XPS analysis showed no significant difference in surface chemistry on the two surfaces (Fig. 6f, g). Thus, the results from the PC membrane experiments clearly demonstrate (1) the pore size of filtration membrane controls the surface roughness, in the form of surface petal-like microstructures, on the bottom surface of the so-produced rGO membrane; (2) with suitable pore size, surface petal-like microstructures are resulted in on the bottom surface of rGO membrane, which mimics the surface pore structures and thus is the physical imprints of the filtration membrane; (3) the surface petal-like microstructures, once present, induces strong interaction of surface to water, leading to the decreased water receding angle.

**Influence of the asymmetric rGO membrane surfaces on the fog collection behavior**

It has been widely reported that the surface properties of membranes may play a significant effect in their applications, and therefore, when using the asymmetric membranes the surfaces should be carefully considered.[35-38] Here our results demonstrate that the two surfaces of the asymmetric rGO membrane prepared on PVDF membrane substrate exhibited markedly different performance in fog collection, with the top and bottom surfaces achieving efficiency at 260 and 152 $g/m^2 \cdot h$ respectively. The experiment detail is described in *Supporting Information*. Fig. 7 shows quite contrasting behaviors of the captured water droplets on the two surfaces (Video S2 and Video S3), which can be easily explained by their difference in wetting properties. On the bottom surface of the rGO membrane whose receding water contact angle was zero, the captured water droplets gradually coalesced into a water film and were thus hesitant to leave the surface (Fig. 7a). While, on the top surface of the rGO membrane, the captured water droplets tended to coalesce into bigger ones that were later cleared off the surface easily due to the high water receding angle on the surface (Fig. 7b). This result points out that the asymmetric surface properties should be cautiously taken into consideration while designing the surface-related applications for GO and rGO membranes.

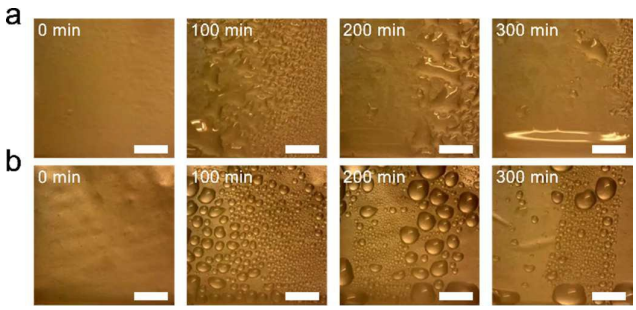


**Fig.7**. Water collection process on two surfaces of the rGO membrane prepared on PVDF substrate. (a). Film-wise water collection process on bottom surface of the rGO membrane. (b). Drop-wise water collection process on top surface of the rGO membrane. The scale bar corresponds to 2 mm.

**Surface engineering of the rGO membrane**

The newfound imprinting mechanism also inspired us to take it to the level of deliberately and selectively engineering only the bottom surface of thin rGO membranes. To this end, we made an effort of creating a silicon wafer with a pre-designed pattern (i.e., KAUST in capital letters) of through-micropore array with pore size at 5.0 μm (Fig. 8a) by lithography and employing it as a filter membrane in the vacuum filtration of GO suspension. Fig. 8b and 8c present the SEM images of the bottom surface of the thus-produced rGO membrane, clearly showing that the exactly the same pattern was faithfully imprinted on the rGO membrane bottom surface and the pattern was made of discrete petal-like microstructures with the diameter around 5.0 μm (Fig. 8d).

Nanoscale Accepted Manuscript

Please do not adjust margins



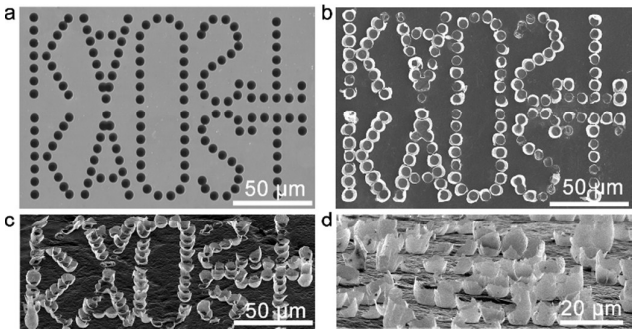


**Fig. 8**. Preparation of patterned microstructure array on rGO membrane. The SEM images of (a) the Si wafer with patterned micropore array, (b) the bottom surface of rGO membrane produced by the Si wafer. (c) Tilted view of the bottom surface of rGO membrane. (d) Cross-sectional view of microstructures on the bottom surface of the rGO membrane.

## Conclusions

In this work, we have revealed the asymmetric wetting behaviors on the two surfaces of the vacuum-filtrated rGO membrane, and have disclosed the asymmetry is originated from the filter membrane's physical imprint on the bottom surface of the rGO membrane. We have revealed that it is the actual surface pore size of the filter membrane that controls its imprinting during the filtration, with the filter membrane imprinting taking place only when the filter surface pores have similar dimension to GO sheets. This work contributes a significant effort to rGO based membrane research as it looks at a generally overlooked side of vacuum-filtration based rGO membrane preparation and provides scientific insight behind it. It also opens up a new avenue of engineering and designing surface micro-structures on rGO membranes by the substrate imprinting concept for potential future applications.

## Acknowledgements

The authors thank Professor Chengzhong (Michael) Yu from the University of Queensland for helpful discussion.

## Notes and references

1. A. K. Geim and K. S. Novoselov, *Nat. Mater.*, 2007, **6**, 183-191.
2. K. S. Novoselov, A. K. Geim, S. Morozov, D. Jiang, Y. Zhang, S. a. Dubonos, I. Grigorieva and A. Firsov, *Science*, 2004, **306**, 666-669.
3. D. R. Dreyer, S. Park, C. W. Bielawski and R. S. Ruoff, *Chem. Soc. Rev.*, 2010, **39**, 228-240.
4. D. Li and R. B. Kaner, *Nat. Nanotechnol.*, 2008, **3**, 101.
5. S. Guo and S. Dong, *Chem. Soc. Rev.*, 2011, **40**, 2644-2672.
6. H. A. Becerril, J. Mao, Z. Liu, R. M. Stoltenberg, Z. Bao and Y. Chen, *ACS Nano*, 2008, **2**, 463-470.
7. Z. Wei, D. Wang, S. Kim, S.-Y. Kim, Y. Hu, M. K. Yakes, A. R. Laracuente, Z. Dai, S. R. Marder and C. Berger, *Science*, 2010, **328**, 1373-1376.
8. J. Zou and F. Kim, *Nat. Commun.*, 2014, **5**.
9. D. Li, M. B. Mueller, S. Gilje, R. B. Kaner and G. G. Wallace, *Nat. Nanotechnol.*, 2008, **3**, 101-105.
10. D. A. Dikin, S. Stankovich, E. J. Zimney, R. D. Piner, G. H. Dommett, G. Evmenenko, S. T. Nguyen and R. S. Ruoff, *Nature*, 2007, **448**, 457-460.
11. G. Eda, G. Fanchini and M. Chhowalla, *Nat. Nanotechnol.*, 2008, **3**, 270-274.
12. H. Liu, H. Wang and X. Zhang, *Adv. Mater.*, 2015, **27**, 249-254.
13. J. N. Coleman, M. Lotya, A. O'Neill, S. D. Bergin, P. J. King, U. Khan, K. Young, A. Gaucher, S. De and R. J. Smith, *Science*, 2011, **331**, 568-571.
14. B. G. Choi, M. Yang, W. H. Hong, J. W. Choi and Y. S. Huh, *ACS Nano*, 2012, **6**, 4020-4028.
15. Y. Han, Z. Xu and C. Gao, *Adv. Funct. Mater.*, 2013, **23**, 3693-3700.
16. M. Hu and B. Mi, *Environ. Sci. Technol.*, 2013, **47**, 3715-3723.
17. C. Wu, X. Lu, L. Peng, K. Xu, X. Peng, J. Huang, G. Yu and Y. Xie, *Nat. Commun.*, 2013, **4**.
18. S. Stankovich, D. A. Dikin, R. D. Piner, K. A. Kohlhaas, A. Kleinhammes, Y. Jia, Y. Wu, S. T. Nguyen and R. S. Ruoff, *Carbon*, 2007, **45**, 1558-1565.
19. Y. Huang, H. Li, L. Wang, Y. Qiao, C. Tang, C. Jung, Y. Yoon, S. Li and M. Yu, *Adv. Mater. Interf.*, 2015, **2**.
20. R. Nair, H. Wu, P. Jayaram, I. Grigorieva and A. Geim, *Science*, 2012, **335**, 442-444.
21. C.-N. Yeh, K. Raidongia, J. Shao, Q.-H. Yang and J. Huang, *Nat. Chem.*, 2015, **7**, 166-170.
22. W. S. Hummers Jr and R. E. Offeman, *J. Am. Chem. Soc.*, 1958, **80**, 1339-1339.
23. L. Zhang, G. Chen, M. N. Hedhili, H. Zhang and P. Wang, *Nanoscale*, 2012, **4**, 7038-7045.
24. Y. Wang, L. Zhang, J. Wu, M. Hedhili and P. Wang, *J. Mater. Chem. A, 2015,**3**, 18963-18969*.
25. J. Zhang, H. Yang, G. Shen, P. Cheng, J. Zhang and S. Guo, *Chem. Commun.*, 2010, **46**, 1112-1114.
26. I. K. Moon, J. Lee, R. S. Ruoff and H. Lee, *Nat. Commun.*, 2010, **1**, 73.
27. R. Raj, S. C. Maroo and E. N. Wang, *Nano Lett.*, 2013, **13**, 1509-1515.
28. D. F. Cheng, C. Urata, M. Yagihashi and A. Hozumi, *Angew. Chem. Int. Ed.*, 2012, **124**, 3010-3013.
29. P. G. Pittoni, C.-H. Lin, T.-S. Yu and S.-Y. Lin, *Langmuir*, 2014, **30**, 9346-9354.
30. A. Nakajima, *NPG Asia Mater.*, 2011, **3**, 49-56.
31. T. Sun, L. Feng, X. Gao and L. Jiang, *Acc. Chem. Res.*, 2005, **38**, 644-652.
32. A. K. Kota, W. Choi and A. Tuteja, *MRS Bullet.*, 2013, **38**, 383-390.
33. K. Haubner, J. Murawski, P. Olk, L. M. Eng, C. Ziegler, B. Adolphi and E. Jaehne, *ChemPhysChem*, 2010, **11**, 2131-2139.
34. E. Drioli and L. Giorno, *Comprehensive membrane science and engineering*, Newnes, 2010.
35. L. Zhang, J. Wu, M. N. Hedhili, X. Yang and P. Wang, *J. Mater. Chem. A*, 2015, **3**, 2844-2852.
36. D. J. Preston, D. L. Mafra, N. Miljkovic, J. Kong and E. N. Wang, *Nano Lett.*, 2015, **15**, 2902-2909.
37. G. T. Kim, S. J. Gim, S. M. Cho, N. Koratkar and I. K. Oh, *Adv. Mater.*, 2014, **26**, 5166-5172.
38. L. Zhang, Z. Zhang and P. Wang, *NPG Asia Mater.*, 2012, **4**, e8.

**Graphical abstract**

Asymmetry of the reduced graphene oxide (rGO) membranes prepared by the commonly used vacuum filtration process is

Nanoscale Accepted Manuscript



Please do not adjust margins

disclosed. When the filter membrane surface pores have similar dimension to GO sheets, the entry of GO sheets into its surface pore space during vacuum filtration can take place, leading to the asymmetry of the rGO membrane.

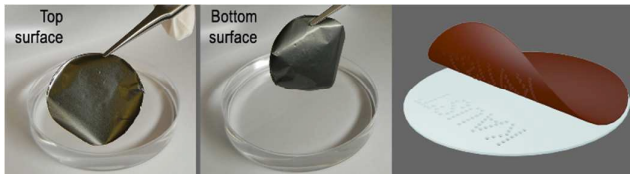


Nanoscale Accepted Manuscript


This journal is © The Royal Society of Chemistry 20xx